Articles

Electron Spin Echo Envelope Modulation Studies of Pyruvate Kinase Active-Site Complexes†

Peter A. Tipton,* John McCracken, Jeffrey B. Cornelius, and Jack Peisach
Department of Molecular Pharmacology, Albert Einstein College of Medicine, Bronx, New York 10461
Received November 14, 1988; Revised Manuscript Received February 21, 1989

ABSTRACT: Electron spin echo envelope modulation (ESEEM) spectroscopy, with Mn^{2+} and VO^{2+} as paramagnetic probes, was used to examine active-site structures at the protein-based divalent cation site of rabbit muscle pyruvate kinase in the presence of substrates, products, and the requisite inorganic cofactors. Two different VO·protein complexes were clearly distinguished, which differed with respect to coordination of the active-site lysine to VO^{2+}. Lysine coordination was sensitive to the presence of pyruvate and phosphoenolpyruvate (PEP) and to the nature of the monovalent cation. In the presence of MgATP and oxalate, a 4-MHz ^{31}P contact interaction was observed, which indicates that the ATP is directly coordinated to Mn^{2+} at the protein-based site. No ^{31}P contact interactions were observed, however, in the presence of PEP. Pyruvate was determined to be a bidentate ligand of VO^{2+}, on the basis of the observation of 2.2- and 5.4-MHz ^{13}C contact interactions between VO^{2+} and [1-^{13}C]pyruvate and [2-^{13}C]pyruvate, respectively. Magnetic coupling between VO^{2+} or Mn^{2+} and ^{23}Na, ^{39}K, and ^{133}Cs was observed, demonstrating the close proximity of the monovalent cation and the protein-based divalent cation.

Mg^{2+} and K^+ have long been recognized to play critical roles as cofactors in numerous enzymatic reactions, and magnetic resonance studies have been instrumental in determining their functions (Cohn & Reed, 1982; Suelter, 1970). Where Mn^{2+} can be substituted for Mg^{2+}, Mn^{2+} electron paramagnetic resonance (EPR)[1] has been used with great success to assign metal ligands and to detect changes in the environment around the metal upon binding of substrates (Reed & Markham, 1984). Recently, the vanadyl cation, VO^{2+}, has been demonstrated to be an effective paramagnetic surrogate for Mg^{2+} (Markham, 1984). VO^{2+}, like Mn^{2+}, offers the advantage of narrow EPR signals and has proven to be an effective probe for detecting the binding of monovalent cations at enzyme active sites (Markham & Leyh, 1987; Lord & Reed, 1987).

The ESEEM[1] technique of pulsed EPR spectroscopy offers great promise for further investigation of the roles of metals in enzymatic reactions. ESEEM resolves superhyperfine interactions that are obscured by the intrinsic line width of the continuous-wave EPR signal. In addition to providing information concerning metal ligation structure, weak superhyperfine interactions between the paramagnetic center and nearby nuclei not bound to the metal can also be observed. Therefore, the metal ion can serve as a probe to investigate the environment beyond its primary coordination sphere. In the past, ESEEM spectroscopy has seen frequent application in studies of Fe and Cu metalloproteins (Mims & Peisach, 1981, 1989). Mn^{2+} ESEEM has only recently been applied to the study of enzyme–substrate complexes (LoBrutto et al., 1986; Eads et al., 1988), and to date, the ability to detect alkali metals by ESEEM spectroscopy has not been exploited nor has VO^{2+} been thoroughly investigated as an ESEEM probe in biological systems. The advantage of ESEEM for the determination of superhyperfine interactions lies in the fact that its usefulness is not limited to samples with narrow EPR resonances, as continuous-wave EPR spectroscopy is, nor is it necessary for ligands to be in rapid exchange, as required for NMR relaxation studies. Therefore, we have undertaken a study of the pyruvate kinase active site in order to characterize the roles of its inorganic cofactors more fully, and to assess the utility of ESEEM spectroscopy in investigations of enzymes which require such cofactors.

Pyruvate kinase is a classic example of a nonmetalloprotein which requires metal ions for activity. This enzyme catalyzes the reversible formation of ATP from phosphoenolpyruvate (PEP) and ADP.

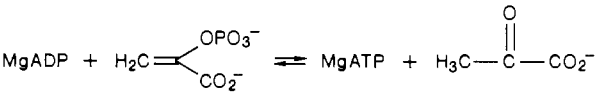

The forward reaction consists of phosphoryl group transfer and a proton transfer from solvent to pyruvate. The observation by Rose (1960) that pyruvate kinase catalyzes the exchange of ^3H from [^{3}H]pyruvate with solvent protons demonstrated that the enzyme catalyzes the enolization of pyruvate and that this proton transfer reaction can be uncoupled from the phosphoryl transfer reaction. In addition, pyruvate kinase has been shown to phosphorylate such diverse substrates as fluoride (Tietz & Ochoa, 1958) and glycolate (Kayne, 1974).

The catalytic reaction of pyruvate kinase requires two divalent metal ions and a monovalent cation, presumably Mg^{2+} and K^+, respectively, in vivo. Like all kinases, pyruvate kinase binds the divalent cation and the nucleotide as a bimolecular complex. A number of independent lines of evidence have demonstrated that a unique binding site exists on the enzyme for a second divalent metal ion. Gupta et al. (1976) inves-

† Supported by NIH Grants GM 40168 and RR 02583. P.A.T. is supported by NIH Postdoctoral Fellowship GM 12081.

[1] Abbreviations: ESEEM, electron spin echo envelope modulation; EPR, electron paramagnetic resonance; PK, pyruvate kinase; PEP, phosphoenolpyruvate; Tris, tris(hydroxymethyl)aminomethane; HEPES, *N*-(2-hydroxyethyl)piperazine-*N*′-2-ethanesulfonic acid; DTT, dithiothreitol.

0006-2960/89/0428-5720$01.50/0

tigated ^3H washout from [^3H]pyruvate in the presence of the exchange-inert complex CrATP and showed that Mg^{2+} or Mn^{2+} was required for proton exchange. Baek and Nowak (1982) demonstrated a synergistic activation of pyruvate kinase by Mn^{2+} and Mg^{2+}, which was interpreted in terms of selectivity by the enzyme for MgADP at the metal–nucleotide site, and for Mn^{2+} at the second (protein-based) site. Pyruvate kinase is active with a number of monovalent cations; activity is maximal in the presence of K^+ and seems to be correlated with the ionic radius of the monovalent cation (Villafranca & Raushel, 1982).

Lodato and Reed (1987) have exploited the divalent metal ion site selectivity with investigations based on observations of inhomogeneous broadening of the Mn^{2+} EPR signal from ^{17}O, which demonstrated that the protein-based metal ion interacts with the γ-phosphate of ATP, and with oxalate, a linear competitive inhibitor versus pyruvate. We have further investigated the coordination of substrates and products to the protein-based metal ion using ESEEM, with Mn^{2+} and VO^{2+}. We have also spectroscopically detected the monovalent cation bound at the active site and observed a ligand exchange reaction at the protein-based metal ion which demonstrates the existence of at least two distinct VO·protein complexes.

Materials and Methods

Rabbit muscle pyruvate kinase was purchased from Boehringer Mannheim; the commercial preparation appeared pure by SDS–PAGE stained with Coomassie blue, and was therefore used without any further purification. The protein was desalted either by dialysis against 50 mM Tris, pH 7.5, or 50 mM HEPES, pH 7.5, or by passage over Sephadex G-25 resin in either of the above buffers. Desalted protein was concentrated with an Amicon Minicon ultrafiltration apparatus, and protein concentration was determined by means of the Bradford assay (Bradford, 1976). Samples used for ESEEM experiments were prepared in a total volume of 0.1 mL; the addition of glycerol, usually added to preserve magnetic dilution in frozen solution, did not improve signal to noise noticeably and was therefore omitted from most protein samples. Model complex samples were prepared in 50% ethylene glycol. All samples were frozen immediately after preparation and were stored at 77 K.

[$^2H_3$]Pyruvate was prepared by the protocol of Attwood et al. (1986) and isolated by chromatography on Dowex 1-x8. [$^2H_3$]Pyruvate was analyzed by ^1H NMR and found to have negligible residual ^1H content. The sodium salts of 99 atom % [1-^{13}C]pyruvate, [2-^{13}C]pyruvate, and [3-^{13}C]pyruvate were purchased from MSD Stable Isotopes and were converted to the potassium salts by chromatography on Dowex 1-x8 using KCl as the eluant. The pyruvates were determined to be pure and specifically labeled by ^{13}C NMR analysis.

$VO(glycinate)_2$ was synthesized by the method of Holyk (1979). $VO(pyruvate)_2$ was prepared by adding a 500-fold excess of pyruvate to 2 mM $VOSO_4$ at pH 2, followed by adjustment of the pH to 7 with NaOH. $VO(imidazole)_4$ was prepared by adding a 100-fold excess of imidazole at pH 2 to 2 mM $VOSO_4$, followed by adjustment of the pH to 8 with NaOH.

ESEEM spectra were obtained with a pulsed EPR spectrometer described by McCracken et al. (1987). Data were obtained near 8.8 and 10 GHz using a folded stripline cavity that is compatible with samples in standard 4-mm EPR tubes (McCracken et al., 1987). To obtain data at 11.5 GHz, a stripline transmission cavity was used (Mims, 1974). Both two-pulse and three-pulse, or stimulated echo, data were collected, usually near $g = 1.85$ or $g = 2.00$. In three-pulse experiments, the value of τ, the time between the first and the second pulse, was chosen to suppress contributions from protons (Mims & Peisach, 1981). VO^{2+} spectra were obtained at 4.2 K, and Mn^{2+} spectra were obtained at 1.8 K. Data sets were composed of 1024 points; each point was separated by 2 or 4 ns in two-pulse experiments and by 10 ns in three-pulse experiments. Each point represented the average of 40–200 individual measurements of the echo amplitude at time τ in two-pulse experiments and at the time $\tau + T$ (where T is the time between the second and third pulses) in three-pulse experiments. Time domain data were analyzed by using the dead time reconstruction protocol of Mims (1984), followed by Fourier transformation. Spectral simulations of $S = {}^1/_2$ systems interacting with $I = 1$ nuclei were carried out by using programs described by Magliozzo et al. (1987); simulations of $S = {}^1/_2$ systems interacting with $I \geq {}^1/_2$ nuclei, where nuclear quadrupole interactions could be ignored, were carried out by using the program described by Snetsinger et al. (1988). All simulations were performed on a Micro Vax II computer.

Results

The spectral characteristics of several enzyme–substrate, enzyme–product, and enzyme–inhibitor complexes are summarized in Table I. These data reveal the nature of substrate and product interactions with the protein-based divalent cation, and the changes in the divalent metal complexes effected by the species bound at the active site.

Vanadyl–Lysine Coordination. In spectra of VO^{2+}-pyruvate kinase complexes with PEP, ^{14}N peaks were observed at 3.8 and 7.2 MHz in data collected at 8.8 GHz and 3130 G (Figure 1A), and at 3.4 and 7.4 MHz in data collected at 10.0 GHz and 3870 G (Figure 1B). Since these spectral lines do not scale linearly with magnetic field, they must arise from magnetic interactions with nuclei where the electron–nuclear coupling is not dominated by dipole or contact interactions. In a metal–protein complex, this type of interaction can arise only from ^{14}N. These ^{14}N interactions are attributed to lysine coordination, based on comparisons with VO^{2+} model complexes. As shown in Figure 1C,D, the spectrum of $VO(glycinate)_2$, selected as an example of coordination to VO^{2+} by a primary amine, appears identical with that observed for enzyme samples at two different microwave frequencies. In contrast, $VO(imidazole)_4$, used as a model for histidine coordination, contains peaks at 2.5, 5.0, and 8.7 MHz in spectra obtained under similar conditions.

Analysis of the ^{14}N ESEEM data obtained for VO–enzyme and $VO(glycinate)_2$ complexes was achieved by using the density matrix formalism of Mims (1972) and the approach discussed by Magliozzo et al. (1987). In general, the superhyperfine splittings for ^{14}N consist of contributions from nuclear Zeeman, electron–nuclear hyperfine, and nuclear quadrupole interactions. For cases where the isotropic portion of the hyperfine interaction (A_{iso}) dominates the magnetic coupling, one often finds that only the transitions between the outer two energy levels from each electron spin manifold (essentially $\Delta m_I = 2$ transitions) are observed (Dikanov et al., 1984). Under these conditions, if data are collected at two different microwave frequencies, reasonably good values for e^2qQ, the nuclear quadrupole coupling constant, and A_{iso} can be obtained from calculations. The ESEEM data obtained for VO–enzyme and $VO(glycinate)_2$, shown in Figure 1, represent such a case. The results of our computer simulation analysis are indicated by the dotted lines in Figure 1 with the coupling parameters being given in the figure caption. The values of A_{iso} obtained for the protein and the model complex are nearly identical (4.9 and 5.0 MHz, respectively), and the

Table I: ESEEM Spectral Characteristics of Pyruvate Kinase Complexes and Model Complexes

sample	H (G)	ν (GHz)	g	υ_{obsd} (MHz)	A_{iso} (MHz)	assignment	calcd Larmor (MHz)
VO·PK·[1-^{13}C]pyruvate	4064	11.382	2.00	3.4, 5.6	2.2	^{13}C	4.4
	3460	8.958	1.85	2.9, 4.9	2.0	^{13}C	3.7
VO·PK·[2-^{13}C]pyruvate	4050	11.341	2.00	1.7, 7.1	5.4	^{13}C	4.4
	3402	8.768	1.84	6.4		^{13}C	3.6
Mn·PK·MgATP·oxalate	3404	8.823	1.85	3.9, 8.0	4.1	^{31}P	5.9
	3860	9.999	1.85	4.4, 8.3	4.1	^{31}P	6.7
VO·PK·K$^+$·PEP	3126	8.836	2.02	3.7, 7.1	4.9[a]	^{14}N	
VO·PK·K$^+$·PEP·P$_i$	3133	8.845	2.02	3.7, 7.0	4.9[a]	^{14}N	
VO·PK·Cs$^+$·PEP	3126	8.792	2.01	1.8		^{133}Cs	1.8
				2.4, 3.8, 7.2	4.9[a]	^{14}N	
VO·PK·Cs$^+$·pyruvate	3148	8.862	2.01	1.8		^{133}Cs	1.8
				2.4, 3.8, 7.2	4.9[a]	^{14}N	
VO·PK·Li$^+$·pyruvate	3166	8.872	2.00	3.8, 7.2	4.9[a]	^{14}N	
VO·PK·Na$^+$·oxalate	3110	8.773	2.02	3.5		^{23}Na	3.5
VO·PK·Na$^+$·pyruvate	3121	8.780	2.01	3.5		^{23}Na	3.5
Mn·PK·Cs$^+$·PEP	3404	8.784	1.84	1.9		^{133}Cs	1.9
Mn·PK·Na$^+$·PEP	3404	8.805	1.85	3.7		^{23}Na	3.8
Mn·PK·Na$^+$·oxalate	3100	8.754	2.02	3.5		^{23}Na	3.5
	3562	10.006	2.01	4.0		^{23}Na	4.0
VO(glycinate)$_2$	3128	8.826	2.02	3.8, 7.3	5.0[a]	^{14}N	
	3600	10.125	2.01	3.6, 7.5	5.0[a]	^{14}N	
VO·PK·pyruvate-d_3	3416	8.845	1.85	2.2		^{2}H	2.2
	3872	10.025	1.85	2.5		^{2}H	2.5
VO([2-^{13}C]pyruvate)$_2$	3128	8.831	2.02	1.2, 3.0, 6.4	5.4	^{13}C	3.3

[a] Based on simulation of experimental data.

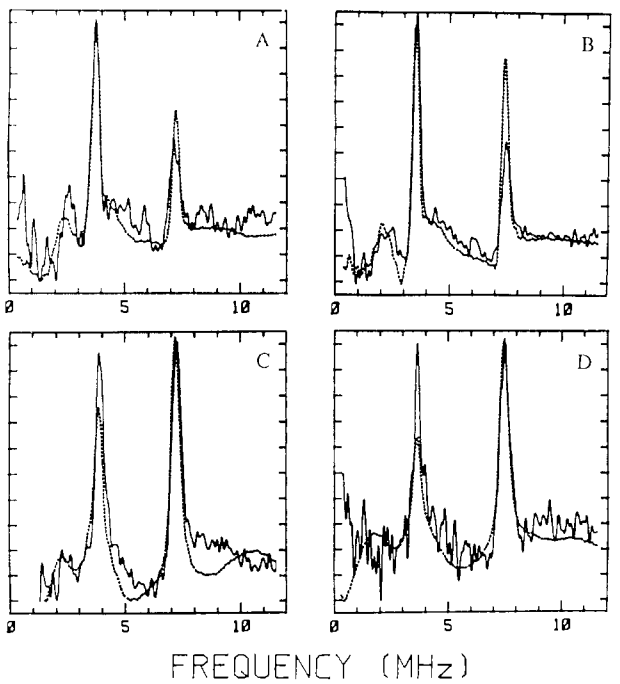

FIGURE 1: Lysine coordination at the active site of pyruvate kinase. Solid lines, experimental data; dotted lines, simulated data. (A) VO·PK·PEP, ν = 8.8 GHz, H = 3130 G. (B) VO·PK·PEP, ν = 10 GHz, H = 3870 G. Parameters for the simulation were $A_{xx} = A_{yy}$ = 4.8 MHz, A_{zz} = 5.1 MHz, e^2qQ = 2.55 MHz, η = 0.5, and number of ^{14}N = 1. (C) VO(glycinate)$_2$, ν = 8.8 GHz, H = 3130 G. (D) VO(glycinate)$_2$, ν = 10 GHz, H = 3870 G. Parameters for the simulation were $A_{xx} = A_{yy}$ = 4.85 MHz, A_{zz} = 5.3 MHz, e^2qQ = 2.55 MHz, η = 0.5, and number of ^{14}N = 2. A_{xx}, A_{yy}, and A_{zz} are the principal values of the hyperfine coupling tensor, e^2qQ is the quadrupole coupling constant, η is the asymmetry parameter, ν is the microwave frequency, and H is the magnetic field strength.

value of e^2qQ, 2.55 MHz, is consistent with those normally observed for an unprotonated amine nitrogen (Lucken, 1969). It should be noted that the ^{14}N peaks observed at g = 2 at 8.8 GHz are centered exactly around the ^{31}P Larmor frequency at this magnetic field strength, and so might be mistakenly assigned to contact-shifted ^{31}P resonances. This underscores the importance of determining the field dependence of signals by obtaining data at two microwave frequencies to avoid errors in signal assignment.

Pyruvate kinase was observed to form two distinct complexes distinguishable by VO^{2+} ESEEM. In one complex, modulations arising from ^{14}N directly coordinated to VO^{2+} were observed; in the other complex, no ^{14}N interactions with VO^{2+} were apparent. All VO^{2+} spectra of enzyme–PEP complexes contained ^{14}N modulations; in contrast, the presence of ^{14}N modulations in enzyme–pyruvate complexes was sensitive to the nature of the monovalent cation. ^{14}N modulations identical with those observed in enzyme–PEP complexes appeared in spectra of VO·PK·Cs$^+$·pyruvate and VO·PK·Li$^+$·pyruvate. ^{14}N modulations were not apparent in spectra of VO·PK·Na$^+$·pyruvate, nor were they apparent in spectra of VO·PK·K$^+$·pyruvate taken immediately after mixing. If, however, the sample was thawed and incubated at room temperature, ^{14}N modulations slowly appeared (Figure 4), suggesting that a slow isomerization was occurring.

Phosphate Coordination to the Divalent Cation. The nature of the interaction between the protein-based divalent cation and ATP was revealed by the ^{31}P signals observed in Mn^{2+} ESEEM spectra. Two-pulse spectra of Mn·PK·MgATP·oxalate obtained at 9.9 GHz revealed two ^{31}P peaks at 4.4 and 8.3 MHz, which are centered around the ^{31}P Larmor frequency of 6.7 MHz, with an isotropic hyperfine coupling constant of 4.4 MHz (Figure 2). As indicated in Table I, data obtained at a lower microwave frequency corroborate this assignment in that the center position of the doublet scales with the magnetic field, while A_{iso}, the hyperfine coupling constant, remains 4.1 MHz. Observation of this contact interaction demonstrates direct coordination between Mn^{2+} and a phosphoryl group of ATP (LoBrutto et al., 1986). These signals were clearly observed in two-pulse experiments, while only the low-frequency component of the ^{31}P doublet was resolved by stimulated echo measurements.

No convincing evidence could be adduced for coordination of the phosphoryl group of PEP to Mn^{2+}. From these results, we cannot, of course, distinguish between an absence of phosphate coordination to Mn^{2+} and an inability to detect

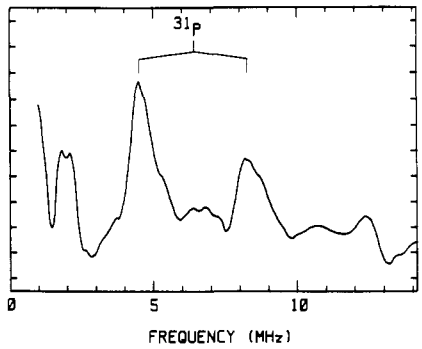

FIGURE 2: Two-pulse spectrum of Mn·pyruvate kinase·MgATP·oxalate; H = 3880 G, ν = 9.999 GHz. The sample contained 2.0 mM pyruvate kinase active sites, 0.8 mM $Mn(OAc)_2$, 5 mM oxalate, 60 mM KCl, 1.7 mM ATP, and 2.0 mM $Mg(OAc)_2$.

coordination by ESEEM. If PEP were coordinated to Mn^{2+}, and the magntidue of the magnetic interaction was similar to that seen in Mn–ATP and Mn–pyrophosphate, there is no reason why ^{31}P contact interactions would not be apparent. Since optimum nuclear-state mixing occurs when $A_{iso}/2$ is equal to the nuclear Zeeman frequency (Flanagan & Singel, 1987; Mims & Peisach, 1978), ^{31}P interactions might not be detected if the hyperfine coupling constant was less than 4 MHz, unless the data were collected at microwave frequencies below X band.

Pyruvate Coordination to the Divalent Cation. Two-pulse spectra of VO^{2+}–enzyme complexes with ^{13}C-labeled pyruvates are shown in Figure 3. ^{13}C contact interactions with VO^{2+} are clearly seen in the spectrum of the VO·PK·[1-^{13}C]pyruvate complex (Figure 3A); the peaks, separated by a contact interaction of 2.2 MHz, at 3.4 and 5.6 MHz are centered around the ^{13}C Larmor frequency of 4.4 MHz. The negative peak near 9.0 MHz is a ^{13}C sum frequency line (Mims, 1972). The data are not as clear with [2-^{13}C]pyruvate, where a signal appears at 7.1 MHz, because the hyperfine coupling constant appears to be larger, about 5.4 MHz, so that the contact-shifted peaks are obscured by the ESEEM background decay at low frequency, and the ^{13}C sum frequency line at high frequency (Figure 3B). However, our assignment is supported by the observation that the 7.1-MHz peak moves to 6.4 MHz when the magnetic field and microwave frequency are decreased (although the low-frequency component of the ^{13}C doublet becomes completely lost in the background decay) (Figure 3C), the appropriate scaling of the ^{13}C sum frequency line with magnetic field, and by comparison with the spectrum of VO([2-^{13}C]pyruvate)$_2$ (Figure 3D) in which both components of the ^{13}C doublet are resolved, at 1.2 and 6.4 MHz, as well as a peak at 3.0 MHz, the Larmor frequency of ^{13}C.

Dipole interactions between the ^2H on [$^2H_3$]pyruvate and VO^{2+} are clearly observed as a peak at 2.2 MHz (Figure 4). Simulation of these spectra, assuming point dipole interactions, yielded an apparent VO^{2+}–deuterium distance of 4.0 Å.[2]

The Monovalent Cation. Several different alkali metals will bind at the active site of pyruvate kinase, and their presence could be detected in ESEEM spectra. VO·PK·oxalate and Mn·PK·oxalate complexes prepared in solutions containing Na^+ as the counterion showed a signal at the Larmor frequency of ^{23}Na (Figure 5A,B). This signal was absent in spectra of samples prepared with K^+ as the counterion. ^{39}K

[2] Model building suggests that the distance between VO^{2+} and the methyl protons of pyruvate should be closer to 4.8 Å. As pointed out by one reviewer, an accurate distance estimate would require a sophisticated analysis of the contribution from spin density on C-2 to the dipolar interaction.

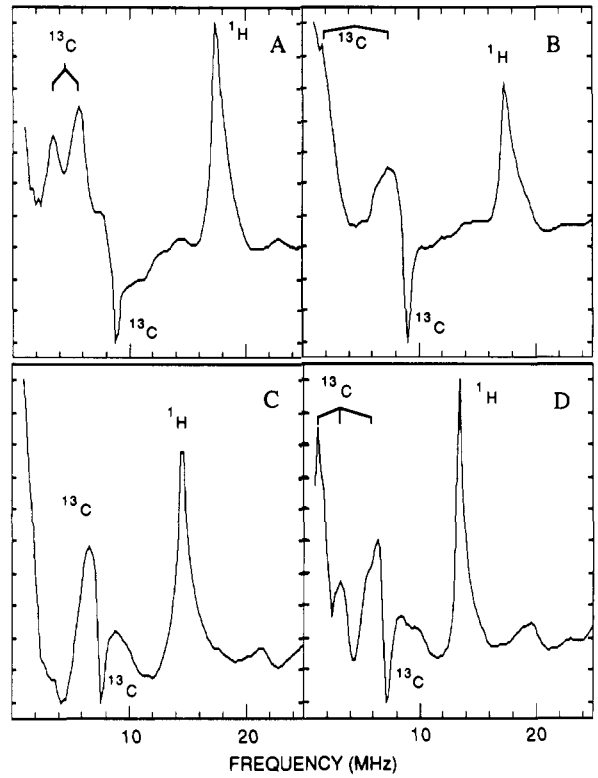

FIGURE 3: (A) Two-pulse spectrum of VO·pyruvate kinase·[1-^{13}C]-pyruvate obtained at 11.4 GHz, H = 4060 G. The sample contained 2.1 mM pyruvate kinase active sites, 6 mM [1-^{13}C]pyruvate, 1.4 mM $VOSO_4$, 200 mM KCl, and 1 mM DTT. (B) Two-pulse spectrum of VO-pyruvate kinase·[2-^{13}C]pyruvate obtained at 11.3 GHz, H = 4050 G. The sample contained 1.3 mM pyruvate kinase active sites, 1.0 mM $VOSO_4$, 5.1 mM [2-^{13}C]pyruvate, 43 mM potassium phosphate, and 1 mM DTT. (C) The same sample as in (B), but data were obtained at 8.8 GHz, H = 3400 G. (D) Two-pulse spectrum of 1 mM VO([2-^{13}C]pyruvate)$_2$ in 50% ethylene glycol, obtained at 8.8 GHz, H = 3130 G. The peaks at high frequency arise from matrix ^1H's.

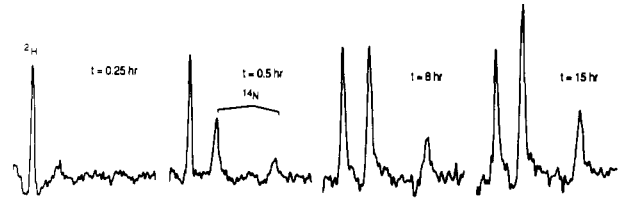

FIGURE 4: Three-pulse spectra of VO·PK·[$^2H_3$]pyruvate; H = 3416 G, ν = 8.845 GHz. The sample contained 1.1 mM pyruvate kinase active sites, 0.7 mM $VOSO_4$, 6.5 mM [$^2H_3$]pyruvate, 50 mM KCl, and 1 mM DTT. After each spectrum was obtained, the sample was thawed and incubated at room temperature until the next time point, when it was frozen in liquid nitrogen. The ^2H signal appears at 2.2 MHz; ^{14}N signals appear at 3.8 and 7.2 MHz.

is difficult to detect directly because its small magnetic moment leads to a very low Larmor frequency at the field strengths routinely used for X-band measurements. Therefore, the ^{39}K signal was obscured by the background decay of the data and was resolved only upon removal of the background decay function. This was achieved by taking the ratio of the data obtained for VO·PK·Na^+·pyruvate and the data obtained for VO·PK·K^+·pyruvate using the procedure outlined by Mims et al. (1984). The result is shown in Figure 5C where the ^{23}Na and ^{39}K resonances, which represent the only detectable differences between the two samples, appear at 3.5 and 0.6 MHz, respectively.

^{23}Na and ^{133}Cs modulations were also visible in Mn^{2+} and VO^{2+} spectra of enzyme complexes with pyruvate and PEP. ^{133}Cs modulations endure for almost 10 μs in three-pulse experiments, leading to an extremely narrow peak in the Fourier

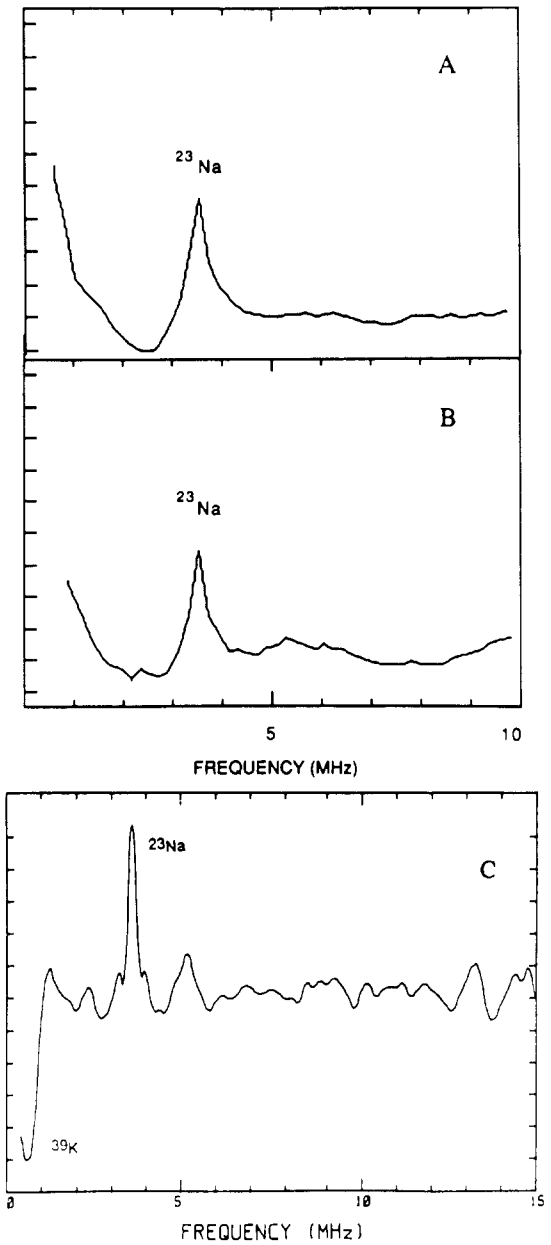

FIGURE 5: (A) Three-pulse spectrum of Mn·pyruvate kinase·Na^+·oxalate; H = 3100 G, ν = 8.754 GHz. The sample contained 0.8 mM pyruvate kinase active sites, 0.7 mM $MnCl_2$, 20 mM oxalate, and 75 mM NaCl. (B) Three-pulse spectrum of VO·pyruvate kinase·Na^+·oxalate; H = 3110 G, ν = 8.773 GHz. The sample contained 0.8 mM pyruvate kinase active sites, 0.7 mM $VOSO_4$, 20 mM oxalate, 75 mM NaCl, and 1 mM DTT. (C) Fourier transform of the data set obtained by dividing time domain data for the VO·pyruvate kinase·K^+·oxalate complex into data for the VO·pyruvate kinase·Na^+·oxalate complex.

transform. The ^{133}Cs Larmor line appears at 1.75 MHz in spectra of the VO·PK·Cs^+·pyruvate and VO·PK·Cs^+·PEP complexes (Figure 6). The other peaks in these spectra are assigned to ^{14}N and are discussed below.

Because VO^{2+} is an $S = {}^1/_2$ paramagnet and only the nuclear Zeeman and electron–nuclear hyperfine interactions need to be considered for these alkali metal ions bound to pyruvate kinase, the data are amenable to further analysis by spectral simulation. However, attempts to simulate the ^{23}Na and ^{133}Cs modulation patterns observed in several spectra proved to be more complicated than we had anticipated. Experimental data were prepared for comparison with simulated data by generating a frequency domain spectrum using dead-time reconstruction and Fourier transformation; a region around the

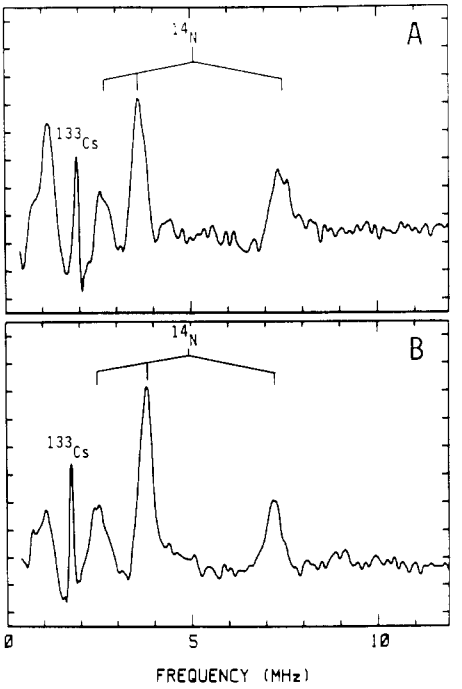

FIGURE 6: (A) Three-pulse spectrum of VO·pyruvate kinase·Cs^+·pyruvate; H = 3148 G, ν = 8.862 GHz. The sample contained 2.2 mM pyruvate kinase active sites, 1.6 mM $VOSO_4$, 5 mM pyruvate, 75 mM CsCl, and 1 mM DTT. (B) Three-pulse spectrum of VO·pyruvate kinase·Cs^+·PEP; H = 3126 G, ν = 8.792 GHz. The sample contained 1.6 mM pyruvate kinase active sites, 1.2 mM $VOSO_4$, 5 mM PEP, 75 mM CsCl, and 1 mM DTT.

peak of interest was then back-transformed to generate a time domain modulation pattern which was used for comparison with simulated data. Difficulties arose when it became apparent that the modulation pattern generated by the back-transform still contained elements of the echo envelope decay function which affected the damping of the modulation pattern. A further complication stems from the fact that the width of the region that is back-transformed can critically affect the damping of the resultant modulation function.

We were able to overcome these complications for simulations of the ^{23}Na modulation from VO·PK·Na^+·oxalate complexes by taking the ratio of the VO·PK·Na^+·oxalate modulation envelope and the modulation envelope obtained for the VO·PK·K^+·oxalate complex. To the extent that these complexes have the same decay functions, this manipulation removes the decay, as well as contributions from other magnetic nuclei present in both samples, and modulations arising solely from ^{23}Na dominate the new data set. Fourier transformation of these data followed by back-transformation of the ^{23}Na peak yields the data shown in Figure 7A (solid line), along with the simulation of these data (dotted line). Optimal agreement between the experimental data and the simulated data was obtained by using a VO^{2+}–Na^+ distance of 4.8 Å and an isotropic hyperfine coupling constant of 0.05 MHz. Figure 7B shows the Fourier transform of the original experimental data obtained from the ratio of the VO·PK·Na^+·pyruvate and VO·PK·K^+·pyruvate data sets (solid line), and Fourier transform of the back-transform which is shown in Figure 7A (dotted line). It is apparent that little, if any, distortion of the ^{23}Na modulation pattern has been introduced by the back-transformation manipulation. Changing the width of the region that was back-transformed by several tenths of a megahertz caused about a 0.2-Å change in the estimate of the VO^{2+}–Na^+ distance.

Cs^+ modulation data could not be treated in the same manner as the Na^+ data, because a data set suitable for di-

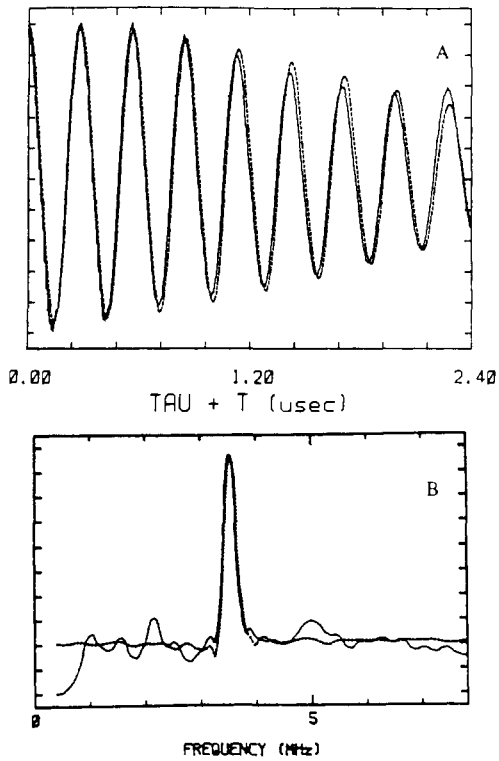

FIGURE 7: (A) ^{23}Na modulation pattern obtained by taking the ratio of the VO·PK·Na^+·pyruvate and VO·PK·K^+·pyruvate modulation patterns (solid line), and the simulation of these data (dotted line), using a VO^{2+}–Na^+ distance of 4.5 Å and A_{iso} = 0.05 MHz. (B) Fourier transform of the ratio of the VO·PK·Na^+·pyruvate and VO·PK·K^+·pyruvate envelope modulations (solid line) and of the modulation pattern obtained by back-transforming the region around the ^{23}Na peak (dotted line). Experimental data were obtained at H = 3121 G, ν = 8.780 GHz.

viding into the Cs^+ data set was not available; therefore, the decay function could not be removed from the envelope modulation. Because of this, the damping of the Cs^+ modulation pattern obtained via back-transformation of the frequency domain spectrum was more sensitive to the width of the region back-transformed than was the Na^+ modulation pattern. There is, therefore, a certain degree of subjectivity involved in the Cs^+ data analysis, since there is no a priori means of deciding how wide a region should be back-transformed. (Although the simplest way to treat this problem is to back-transform a wide region around the peak of interest, we could not treat the Cs^+ data this way, because a wide window would encompass frequencies from other nuclei.) This results in a very large uncertainty in the estimation of A_{iso}; however, the depths of the modulations at early times are not seriously affected by the decay function (Mims et al., 1982), and one can therefore obtain fairly reliable estimates of the distance between VO^{2+} and Cs^+. From simulations of the Cs^+ modulation patterns in VO·PK·Cs^+·pyruvate and VO·PK·Cs^+·PEP, we concluded that the Cs^+ lies about 6.5 Å from the VO^{2+}.

Discussion

The role of Mg^{2+} in enzyme systems has often been studied by substitution of Mn^{2+} for Mg^{2+}. This substitution allows one to apply EPR techniques as well as NMR relaxation techniques. Mn^{2+} offers several advantages for ESEEM studies. First, because most Mg^{2+}-requiring enzymes are active with Mn^{2+} as well, it is reasonable to believe that Mn^{2+}–ligand interactions observed spectroscopically are analogous to Mg^{2+}–ligand interactions which occur in the normal catalytic reaction. Second, Mn^{2+} yields large echoes in pulsed EPR experiments, presumably as a consequence of its relatively narrow EPR absorption envelope and its long phase-memory time. Concentrations as low as 200 μM can be detected easily. Since ESEEM studies require that the protein be present in excess of the metal ion to ensure that all the metal ion is bound, this feature becomes important in instances where the protein is not available in large quantities or has low solubility. Equally useful is the fact that at 1.8 K relaxation of the electron spin magnetization is very rapid; fast cycling times can therefore be used, so signal averaging becomes a viable means for improving signal to noise.

To our knowledge, VO^{2+} has not previously been used in ESEEM investigations as a surrogate of Mg^{2+}, although it has several properties which make it very useful for these studies. The depth of the modulations in the echo envelope is generally greater than that seen with Mn^{2+}. In this study, ^{13}C contact interactions, which were difficult to detect for Mn^{2+}–enzyme complexes, could be resolved in VO^{2+} spectra. Furthermore, because VO^{2+} is an $S = {}^1/_2$ paramagnet, the analysis of spectra is more straightforward, and detailed information can be derived from the observed superhyperfine coupling constants.

Detection of VO^{2+} echoes requires approximately 5-fold higher concentrations of VO^{2+} than is required for detection of Mn^{2+}, for reasons that are not clear. One possibility is that we are simply unable to keep all the added VO^{2+} in solution as VO^{2+}, due to oxidation and formation of EPR-silent aggregates (Chasteen, 1981). Because electron T_1's were long, data had to be collected with cycling times as much as 10-fold longer than those used with Mn^{2+}. Also, VO^{2+} does not support the catalytic activity of many enzymes, so one must exercise some caution in relating spectroscopic results to the active Mg^{2+}-supported system.

The results of several mechanistic and spectroscopic studies of pyruvate kinase suggest a reasonable hypothesis for the function of the protein-based divalent cation, namely, that it coordinates to the phosphoryl group that is transferred from PEP to MgADP during catalytic turnover. Spectra of the quaternary complexes Mn^{2+}·PK·MgATP·oxalate had peaks centered around the ^{31}P Larmor frequency with isotropic superhyperfine coupling constants of 4 MHz, in agreement with the value of A_{iso} for coordinated phosphate obtained in crystalline sodium pyrophosphate doped with Mn^{2+} (LoBrutto et al., 1986). The ESEEM data, which clearly indicate direct coordination of phosphate, do not distinguish which of the three phosphate groups of ATP is coordinated to the metal; however, Lodato and Reed (1987) have determined that it is the γ-phosphate based on their observation of inhomogeneously broadened Mn^{2+} EPR lines in the presence of [γ-^{17}O]ATP. These data suggest that phosphate coordination to the divalent cation obtains at the conclusion of the catalytic cycle. Phosphoryl transfer has been found to proceed with inversion of configuration at phosphorus (Blättler & Knowles, 1979), indicating that the reaction proceeds by an associative mechanism in which the metal ion might be imagined to stabilize the pentacoordinate phosphorus transition state via electrostatic interactions. Also, studies of the pH dependence of kinetic parameters (Dougherty & Cleland, 1985) demonstrated that pyruvate kinase binds the trianions of the slow substrates phosphoglycolate and phosphoenolketobutyrate preferentially over the dianions, consistent with the idea that the phosphoryl group must be fully ionized so it can enter the coordination sphere of the metal ion during turnover.

A great deal of effort has therefore been expended in order to garner direct evidence for coordination of PEP to the divalent cation. Mn^{2+} EPR studies with [^{17}O]PEP analogous

to the studies which identified the γ-phosphate of ATP as a ligand, based on the observation of broadening of the Mn^{2+} lines due to superhyperfine interactions with ^{17}O, are not possible because the EPR line widths of the Mn·enzyme·PEP complex are too broad. NMR relaxation studies with PEP and PEP analogues aimed at determining the nature of the coordination to the phosphoryl group have given inconclusive results. Nowak and Mildvan (1972), studying phosphoglycolate, and James and Cohn (1974), studying α-[(dihydroxyphosphinyl)methyl]acrylate, concluded that both of these PEP analogues formed inner-sphere complexes with Mn^{2+}, although James and Cohn cautioned against extrapolating their results to PEP because the ternary complex Mn–pyruvate kinase–α-[(dihydroxyphosphinyl)methyl]acrylate had EPR characteristics very distinct from those observed for Mn·pyruvate kinase·PEP. NMR relaxation studies with Mn^{2+} and PEP itself were not possible because of chemical exchange limitations. Melamud and Mildvan (1975) attempted to circumvent this limitation by using Co^{2+} as the paramagnetic perturbant, since its paramagnetic relaxation rate was slower than the chemical exchange rate of PEP. On the basis of these studies, they concluded that the phosphorus of PEP was 5 Å from Co^{2+}, too far away to be an inner-sphere ligand. Cohn and Reed (1982) have noted, however, that tightly bound substrates directly coordinated to a metal are difficult to recognize using NMR relaxation methods because the condition that the rate of ligand exchange, $1/\tau$, be much faster than $1/T_1$ becomes increasingly difficult to satisfy as the ligand approaches the metal ion, since $1/T_1$ is proportional to r^{-6}.

ESEEM spectra of pyruvate kinase complexes with PEP provide no evidence for coordination of the phosphoryl group of PEP to the protein-based divalent metal ion. As discussed above, this does not represent unequivocal evidence that phosphate coordination does not occur, since the data were not obtained under optimal conditions for detecting ^{31}P contact interactions.

The possibility that the collision complex formed between Mn·pyruvate kinase and PEP does not involve Mn–phosphate coordination does not necessarily contradict the hypothesis discussed above which provides a reasonable role for the protein-based divalent cation. One possible explanation is that binding of MgADP causes local conformation changes that allow the phosphoryl group to enter into the Mn^{2+} coordination sphere. The observation of Reed and Cohn (1973) that the EPR spectrum of Mn·pyruvate kinase does not change upon addition of ADP or ATP argues against this explanation. Also, Nageswara Rao et al. (1979) have determined that the ^{31}P NMR chemical shifts of nucleotides bound to the enzyme are not sensitive to the addition of other substrates, and Nowak (1978) has found that the distance between enzyme-bound Mn^{2+} and $CH_3NH_3^+$ bound at the monovalent cation site does not change upon binding of nucleotides.

Alternatively, the ESEEM data are consistent with a model in which metal–phosphoryl coordination occurs only transiently during the catalytic cycle. Since oxalate is an analogue of the presumed pyruvate enolate intermediate, the Mn·PK·MgATP·oxalate complex is an analogue of an intermediate state along the reaction pathway, and it is not surprising, then, that phosphoryl group coordination is observed.

Although VO^{2+} has been shown to bind to surface residues of proteins in a number of instances (Chasteen, 1981), the observation of ^2H and ^{14}N modulations in spectra of VO·PK·[^{2}H]pyruvate complexes (Figure 4) strongly suggests that VO^{2+} binds at the active site of pyruvate kinase. This conclusion is corroborated by the demonstration that pyruvate kinase exhibits a low level of activity in the presence of VO^{2+} (Lord & Reed, 1984) and by the observation that the magnitude of the $^{205,203}Tl^+$ superhyperfine coupling to VO^{2+} in VO^{2+}–enzyme complexes varies with the presence of different substrates and substrate analogues (Lord & Reed, 1987).

The ESEEM data presented here suggest that there are at least two distinct VO^{2+}–enzyme structures which differ with respect to coordination of the ε-amino group of lysine to VO^{2+}. Dougherty and Cleland (1985) have proposed that an active-site lysine with a pK of 8.3 is responsible for the proton transfer reactions of pyruvate kinase, and Muirhead et al. (1987) have confirmed the presence of lysine in the active site of the cat muscle enzyme by X-ray crystallographic studies. The crystal structure also shows that the lysine is close to the protein-based metal ion, whose ligands in the absence of substrates or products are suggested to be a carboxyl group from Glu-271, the backbone carbonyl oxygens from Ala-292 and Arg-293, and three waters.

Our observation that lysine enters the VO^{2+} coordination sphere under certain conditions demonstrates that its position in the active site is sensitive to the nature of the substrates or products bound. In the presence of PEP, lysine is directly coordinated to the VO^{2+}, regardless of the monovalent cation present (Li^+, Na^+, K^+, Rb^+, Cs^+). This provides a possible explanation for the low catalytic activity of pyruvate kinase in the presence of VO^{2+} (Lord & Reed, 1984). Because the lysine is coordinated to VO^{2+}, it may not be available as a catalytic base to mediate the proton transfer between solvent and the methylene of PEP. The intensity of the ^{14}N lines is invariant with the nature of the monovalent cation, suggesting either that all of the enzyme forms one type of complex (with the lysine coordinated to VO^{2+}) or that the equilibrium between the two complexes is not affected by the monovalent cation. When pyruvate and K^+ are bound, the lysine coordination is not observed in samples frozen immediately after mixing, perhaps because the lysine is in position to abstract the proton from the pyruvate methyl group. This complex slowly isomerizes to a dead-end complex in which the lysine has moved into the coordination sphere of VO^{2+}. Interestingly, formation of this complex seems to be sensitive to the nature of the monovalent cation present. As shown in Figure 4, isomerization occurs only slowly in the presence of pyruvate and K^+. However, when K^+ is replaced by Li^+ or Cs^+, the lysine coordination is evident in samples frozen immediately after mixing. Thus, the monovalent cation has an obvious effect on the formation of the VO·protein complex.

Reed and Cohn (1973) have detected two distinct enzyme–substrate complexes by Mn^{2+} EPR, whose equilibrium is sensitive to the nature of the monovalent cation present. Mn·enzyme·K^+·PEP showed a very anisotropic spectrum; however, when K^+ was replaced by the poor activator, tetramethylammonium cation, the spectrum appeared to be a superposition of the spectrum obtained in the presence of K^+ and the spectrum of the Mn·enzyme·α-[(dihydroxyphosphinyl)-methyl]acrylic acid complex. In contrast to the effects we observed, spectra of Mn·enzyme·pyruvate complexes were not sensitive to the nature of the monovalent cation. Structural differences between enzymes·PEP complexes in the presence of different monovalent cations have also been observed by NMR relaxation techniques. Villafranca and Raushel (1982) have tabulated Mn^{2+} to monovalent cation distances for a series of monovalent cations and have correlated increasing enzyme activity with decreasing distance.

Pyruvate kinase remains the most extensively studied enzyme which requires a monovalent cation for activity. A

number of researchers have applied NMR relaxation techniques (Raushel & Villafranca, 1980b; Ash et al., 1978) and EPR techniques (Lord & Reed, 1987) to determine where the monovalent cation binds and have concluded that the enzyme has a specific binding site for the monovalent cation near the PEP/pyruvate binding site. ESEEM spectroscopy provides a unique means of detecting alkali metal ions, provided they are close enough to the paramagnet for magnetic interactions. Shimizu et al. (1979) first observed ^{23}Na modulations in samples of NdATP prepared from the Na salt of ATP, but since that time, ESEEM spectroscopy has not been exploited for examining the function of alkali metal ions in biological systems.

VO^{2+} proved to be a useful probe for detection of the protein-bound monovalent cations by ESEEM spectroscopy, because simulation of the experimental data yielded estimates of the distance between the divalent and monovalent cations. Simulation of spectra of VO·PK·Na^+·oxalate led to an estimate of 4.8 Å for the VO^{2+}–Na^+ distance, which agrees well with the estimate of ≥4.5 Å obtained by Raushel and Villafranca using NMR relaxation methods to study the Mn·PK·Na^+·PEP complex (Raushel & Villafranca, 1980a).

Simulation of spectra of VO·PK complexes in the presence of Cs^+ and pyruvate or PEP yielded VO^{2+}–Cs^+ distance estimates of 6.5 Å. This is in reasonable agreement with the distance of 6.0 ± 0.3 Å for the Mn^{2+}–Cs^+ distance in Mn·PK·Cs^+·PEP obtained by Raushel and Villafranca (1980a). Presumably, the Cs^+ signal remains easily detectable, in spite of the increased M^{2+}–M^+ distance, relative to Na^+, because of the greater nuclear spin of ^{133}Cs ($S = {}^7/_2$) compared to ^{23}Na ($S = {}^3/_2$). The distance estimates obtained in the presence of Cs^+ and Na^+ suggest that the distance between the monovalent cation and the divalent cation is more sensitive to the nature of the monovalent cation than it is to the nature of the ligands around the divalent metal ion.

It is apparent from the ESEEM data that pyruvate is a bidentate ligand of VO^{2+} in the active site of pyruvate kinase since ^{13}C contact interactions are observed in VO^{2+} spectra of complexes with both [1-^{13}C]pyruvate and [2-^{13}C]pyruvate. We do not yet understand why A_{iso} is different for [1-^{13}C]-pyruvate and [2-^{13}C]pyruvate. The 5-MHz coupling constant observed in VO·[2-^{13}C]pyruvate complexes is of similar magnitude to the superhyperfine coupling observed in Cu([$^{13}C_2$]oxalate)$_2$.[3] Certainly, more data from model complexes will be invaluable in explaining these observations.

From the ESEEM studies emerges a picture of the pyruvate kinase active site as a flexible and dynamic environment. In addition to observing coordination of ligands to the protein-based metal ion, we have determined that the position of the catalytic lysine in the active site is sensitive to the nature of the monovalent cation and to the presence of other species in the active site. Furthermore, the monovalent cation appears to play a role in determining active-site geometries; this effect is manifested by the different M^{2+}–M^+ distances observed with ^{23}Na and ^{133}Cs.

Registry No. PK, 9001-59-6; ATP, 56-65-5; Mn, 7439-96-5; VO^{2+}, 20644-97-7; VO(pyruvate)$_2$, 121013-32-9; $VOSO_4$, 16229-43-9; VO(imidazole)$_4$, 82871-04-3; pyruvate, 127-17-3; imidazole, 288-32-4; L-lysine, 56-87-1.

References

Ash, D. E., Kayne, F. J., & Reed, G. H. (1978) *Arch Biochem. Biophys. 190*, 571.

Attwood, P. V., Tipton, P. A., & Cleland, W. W. (1986) *Biochemistry 25*, 8197.

Baek, Y. A., & Nowak, T. (1982) *Arch. Biochem. Biophys. 217*, 491.

Blättler, W. A., & Knowles, J. R. (1979) *Biochemistry 18*, 3927.

Bradford, M. M. (1976) *Anal. Biochem. 72*, 248.

Chasteen, N. D. (1981) *Biol. Magn. Reson. 3*, 53.

Cohn, M., & Reed, G. H. (1982) *Annu. Rev. Biochem. 51*, 365.

Dikanov, S. A., Astashkin, A. V., & Tsvetkov, Yu. D. (1984) *J. Struct. Chem. 25*, 35.

Dougherty, T. M., & Cleland, W. W. (1985) *Biochemistry 24*, 5875.

Eads, C. D., LoBrutto, R., Kumar, A., & Villafranca, J. J. (1988) *Biochemistry 27*, 165.

Flanagan, H. L., & Singel, D. J. (1987) *J. Chem. Phys. 87*, 5606.

Gupta, R. K., Oesterling, R. M., & Mildvan, A. S. (1976) *Biochemistry 15*, 2881.

Holyk, N. H. (1979) M.S. Thesis, University of New Hampshire, Durham, N.H.

James, T. L., & Cohn, M. (1974) *J. Biol. Chem. 249*, 3519.

Kayne, F. J. (1974) *Biochem. Biophys. Res. Commun. 59*, 8.

LoBrutto, R., Smithers, G. W., Reed, G. H., Orme-Johnson, W. H., Tan, S. L., & Leigh, J. S. (1986) *Biochemistry 25*, 5654.

Lodato, D. T., & Reed, G. H. (1987) *Biochemistry 26*, 2243.

Lord, K. A., & Reed, G. H. (1984) *Biochemistry 23*, 3349.

Lord, K. A., & Reed, G. H. (1987) *Inorg. Chem. 26*, 1464.

Lucken, E. A. C. (1969) *Nuclear Quadrupole Coupling Constants*, Chapter 11, Academic Press, New York.

Magliozzo, R. S., McCracken, J., & Peisach, J. (1987) *Biochemistry 26*, 7923.

Markham, G. D. (1984) *Biochemistry 23*, 470.

Markham, G. D., & Leyh, T. S. (1987) *J. Am. Chem. Soc. 109*, 599.

McCracken, J., Peisach, J., & Dooley, D. M. (1987) *J. Am. Chem. Soc. 109*, 4064.

Melamud, E., & Mildvan, A. S. (1975) *J. Biol. Chem. 250*, 8193.

Mims, W. B. (1972) *Phys. Rev. B5*, 2409.

Mims, W. B. (1974) *Rev. Sci. Instum. 45*, 1583.

Mims, W. B. (1984) *J. Magn. Reson. 59*, 291.

Mims, W. B., & Peisach, J. (1978) *J. Chem. Phys. 69*, 4921.

Mims, W. B., & Peisach, J. (1981) *Biol. Magn. Reson. 3*, 213.

Mims, W. B., & Peisach, J. (1989) in *Advanced EPR in Biology and Biochemistry* (Hoff, A., Ed.) Elsevier, Amsterdam (in press).

Mims, W. B., Davis, J. L., & Peisach, J. (1982) *Biophys. J. 45*, 755.

Muirhead, H., Clayden, D. A., Cuffe, S. P., & Davies, C. (1987) *Biochem. Soc. Trans. 15*, 996.

Nageswara Rao, B. D., Kayne, F. J., & Cohn, M. (1979) *J. Biol. Chem. 254*, 2689.

Nowak, T. (1978) *J. Biol. Chem. 253*, 1998.

Nowak, T., & Mildvan, A. S. (1972) *Biochemistry 11*, 2819.

Raushel, F. M., & Villafranca, J. J. (1980a) *Biochemistry 19*, 5481.

Raushel, F. M., & Villafranca, J. J. (1980b) *J. Am. Chem. Soc. 102*, 6618.

Reed, G. H., & Cohn, M. (1973) *J. Biol. Chem. 248*, 6436.

Reed, G. H., & Markham, G. D. (1984) *Biol. Magn. Reson. 6*, 73.

[3] Feng Jiang, unpublished results, this laboratory.

Rose, I. A. (1960) *J. Biol. Chem. 235*, 1170.
Rowan, L. G., Hahn, E. L., & Mims, W. B. (1965) *Phys. Rev. 137*, A61.
Serpersu, E. H., McCracken, J., Peisach, J., & Mildvan, A. S. (1988) *Biochemistry 27*, 8034.
Shimizu, T., Mims, W. B., Peisach, J., & Davis, J. L. (1979) *J. Chem. Phys. 70*, 2249.
Snetsinger, P. A., Cornelius, J. B., Clarkson, R. B., Bowman, M. K., & Belford, R. L. (1988) *J. Chem. Phys. 92*, 3696.
Suelter, C. H. (1970) *Science 168*, 789.
Tietz, A., & Ochoa, S. (1958) *Arch. Biochem. Biophys. 78*, 477.
Villafranca, J. J., & Raushel, F. M. (1982) *Fed. Proc., Fed. Am. Soc. Exp. Biol. 41*, 2961.

Thiol and Amino Analogues as Alternate Substrates for Glycerokinase from *Candida mycoderma*†

W. B. Knight‡ and W. W. Cleland*

Institute for Enzyme Research and Department of Biochemistry, University of Wisconsin, Madison, Wisconsin 53706

Received January 4, 1989; Revised Manuscript Received April 5, 1989

ABSTRACT: The kinetic and catalytic mechanism of glycerokinase from *Candida mycoderma* was examined with thiol and amino analogues of glycerol and with MgAMPPCP, an analogue of MgATP. (*S*)-1-Aminopropanediol was phosphorylated on nitrogen (V_{max} 0.4% that of glycerol) while the *R* enantiomer was phosphorylated on oxygen (V_{max} 0.7% that of glycerol). (*S*)-1-Mercaptopropanediol was phosphorylated on oxygen (V_{max} 3.5% that of glycerol), while the *R* enantiomer was phosphorylated on sulfur (V_{max} 0.001% that of glycerol). The hydroxyl group at C-2 thus orients the substrate in the active site, while that at the carbon remote from phosphorylation enhances both catalysis and binding of the substrate, presumably because of hydrogen-bonding interactions. The kinetic mechanism is random with a high degree of synergistic binding between the substrates, so that the mechanism appears ordered with glycerol adding first but equilibrium ordered with MgATP binding first with the amino analogues.

Glycerokinase catalyzes the phosphorylation of glycerol by MgATP to produce L-glycerol 3-phosphate (the *R* enantiomer) in a classic example of the ability of an enzyme to distinguish between chemically identical functional groups in a prochiral molecule. From their studies with fluoro analogues of glycerol, Eisenthal et al. (1972) proposed that all three hydroxyls of glycerol are involved in the substrate recognition process. We have examined the roles of the primary hydroxyls in both catalysis and binding by examining the effects of replacement with either thiol or amino groups. On the basis of studies with alternate substrates and dead-end inhibitors, Janson and Cleland (1974) concluded that glycerokinase had an ordered kinetic mechanism with glycerol adding before MgATP. However, these studies would not have distinguished a truly ordered mechanism from a random one with a high degree of synergistic binding between the substrates, and just such a highly synergistic random mechanism has been found for yeast hexokinase by Viola et al. (1982). We have examined the order of addition of substrates to glycerokinase and the degree of synergistic binding by using dead-end inhibitors, by using alternate substrates, and by measuring the MgATPase activity in the presence and absence of a second substrate. Glycerokinase from different sources has been reported to show nonlinear reciprocal plots for MgATP (Thorner & Paulus, 1973), interpreted as either two types of MgATP binding or negative cooperativity. We have explored this possibility with the enzyme from *Candida mycoderma*. We have also examined the pH dependence of the phosphorylation of glycerol and its thiol and amino analogues.

Materials and Methods

Materials. Buffers were titrated to the desired pH with KOH. (*R,S*)-1-Mercapto-2,3-propandiol and (*R,S*)-1-amino-2,3-propanediol from Sigma and Aldrich when used as substrates displayed a burst caused presumably by contaminating glycerol. The thiol from Aldrich and Sigma contained 0.7% and 2%, respectively, while the amine from Aldrich contained 0.5% fast-reacting material. Incubation of these compounds with glycerokinase, MgATP, pyruvate kinase, and phosphoenolpyruvate at pH 7.5 followed by Amicon filtration yielded products free of contamination. (*R,S*)- as well as (*R*)- and (*S*)-2,2-dimethyl-1,3-dioxolane was from Aldrich. AMPPCP, AMPPNP, NAD, and NADH were from Boehringer. Glycerokinase from *Candida mycoderma* or *Escherichia coli* was from Sigma and was dialyzed vs 20 mM Hepes, 5 mM dithiothreitol, and 0.3 mM EDTA, followed by several changes of 20 mM Hepes and 5 mM dithiothreitol, prior to use, and was stored under nitrogen. All other coupling enzymes and high-purity sucrose were from Sigma.

Methods. ^{31}P and ^{13}C NMR spectra were obtained on either Nicolet NT-200 or Bruker AM500 NMR spectrometers while proton NMR spectra were obtained on the NT-200, or on a Bruker WH270 instrument. ^{31}P NMR chemical shifts are referenced to external 200 mM D_3PO_4, while proton and ^{13}C chemical shifts are referenced to external TMS.

Analogue Syntheses. (*R,S*)-1-Mercaptopropanediol 1-phosphate was synthesized from glycerol by tosylation and

† Supported by NIH Grants GM 18938 and GM 09677. A portion of this work was reported by Knight and Cleland (1985).
‡ Present address: Department of Enzymology, Merck Sharp & Dohme Research Laboratories, P.O. Box 2000, Rahway, NJ 07060.

0006-2960/89/0428-5728$01.50/0